

# Image Analysis and Cytometry in Three-Dimensional Digital Reconstruction of Porcine Native Aortic Valve Leaflets

Chi Zheng, M1 - University of Pittsburgh; BSE - University of Michigan  
In association with: John A. Stella and Michael S. Sacks, Ph. D.  
Department of Bioengineering, University of Pittsburgh

June.16.2006

## Introduction

The mammalian heart is a four-chambered pulsating pump that circulates the blood within two parallel loops: the systemic and the pulmonary circulation. Blood flow is regulated by four pressure-sensitive valves that are located at the outlet of the four chambers. In the duration of a complete cardiac cycle, oxygenated blood first enters the left atrium from the pulmonary circulation. It flows past the mitral valve into the left ventricle. The left ventricle contracts, causing the mitral valve to close and the aortic valve to open, resulting in the ejection of oxygenated blood from the ventricle, through the aortic artery, and into the systemic circulation. After delivering oxygen to the tissues, deoxygenated blood returns to the right atrium of the heart. It, then, flows into the right ventricle passing the tricuspid valve in the process. When the right ventricle contracts, the tricuspid valve closes and blood is ejected through the pulmonary valve into the pulmonary vein, which carries the deoxygenated blood to the lungs to be oxygenated. The synchrony of heart muscle contraction and relaxation along with the opening and closing of each valve maintains the quasi-steady state blood flow necessary for mammalian life.

During the lifetime of an average person, each of four valves opens and closes approximately  $3 \times 10^9$  times. [1] Under such physically demanding conditions, the valves are subjected to a number deteriorating conditions such as stenosis from calcification, regurgitative leakage from biomechanical fatigue, bacterial infections, and congenital defects. Improper functioning of the valves could cause heart conditions that lead to abnormal cardiac output, ventricular hypertrophy, and ultimately, heart

failure. Surgical replacement of the damaged valve is required to prevent such catastrophic failures. Of the four aforementioned valves, the aortic valve is the one that most commonly requires replacement.

Currently, there exist two major types of prosthetic valves in the replacement procedure: mechanical and biological. Mechanical prosthetic valves are constructed from synthetic materials such as metal alloys, carbon and various plastic polymers. Biological valves are altered human and animal valves such as porcine aortic valve or bovine pericardium. [2] Each of the two prosthetics offer their distinct advantages and disadvantages. Mechanical prostheses are more durable, lasting around 20 years, but the accumulation of blood clots interferes with their normal function. Biological prostheses are more biocompatible but they carry a replacement rate of 60% after 10 years. [3] Furthermore, neither of the two non-viable prostheses offer the growth-potential required by pediatric patients suffering from congenital valve defects. Hence, the field of tissue engineering is called upon to provide a durable yet viable, immunologically compatible and thromboembolically suitable alternative that meets the needs of pediatric patients. Such a tissue engineered alternative could involve incubated cells integrated into polymer scaffolds. Regardless of its composition, the tissue engineered valve must adequately mimic the performance of the native aortic valve. Therefore, the structure and the biomechanical response of the native valve must be understood and used to serve as the standard for the tissue engineered valve design.

In terms of macrostructure, the aortic valve leaflet is composed of three cell layers: fibrosa, spongiosa, and ventricularis. The fibrosa, facing the lumen of the aorta, contains primarily collagen. The spongiosa, a middle, non-load-carrying layer, is composed mainly of glycosaminoglycans and water. The layer facing the inside of the ventricle, hence the name ventricularis, is composed of

mostly elastin with some collagen. The spongiosa allows for the shearing of the ventricularis against the fibrosa during the ejection phase of the cardiac cycle. Due to the high collagen content and the thickness of the fibrosa (0.4mm) compared to the ventricularis (0.2mm), the fibrosa is considered to bear most of the pressure load imposed on the aortic valve during isovolumetric contraction and relaxation, when all valves are closed and a large pressure gradient exists across the aortic valve. [4] Research has suggested that the elastin fibers, especially in the ventricularis, serve to return the valve leaflets to their natural curvature. [5] Elastin fibers are more elastic and allow for a higher degree of strain than collagen. Figure 1 (see Attachments) shows the possible collaborative microstructure between collagen and elastin in an aortic valve leaflet.

Research has also yielded uniaxial and biaxial mechanical data on the native aortic valve as well as tissue engineered valves. Figure 2 shows the biomechanical response of a porcine native aortic valve leaflet with application of biaxial tension. The “toe” region in the figure represents the delayed response that results from collagen fiber realignment. With initial application of tension, the fibers realign quickly to handle further increase in tension. This type of response pattern is also shown by small angle light scattering (SALS) analysis. [1]

While both the structural and mechanical aspects of the aortic valve leaflet has been studied on a global scale. There still exists a need to visualize the valve leaflet in terms of its regional variability. The goal is to construct a three-dimensional volumetric rendition of the valve leaflet showing heterogeneity in cell count, cell layer thickness, and collagen and elastin content and orientation. To do this, representative sampling of histological slides must be taken at various locations of the leaflet. These sample images must be quantified in terms cytometry, cell layer thickness, and fiber content. After this detailed characterization, the images must be stacked to reconstruct the three-

dimensional representation of the valve leaflet. The following section details the methodology for the cytometric and layer-thickness quantification necessary to construct the three-dimensional rendition of the aortic valve leaflet using bright-field microscope slides and the Image J software supplied by NIH (<http://rsb.info.nih.gov/ij/>).

## **Methods**

Cytometry and quantification of cell layer thickness will be performed for two native porcine aortic valve leaflets. The tissues are extracted from the right coronary leaflets of two separate porcine aortic valves. Each valve is sectioned into 200-400 slices along the circumferential direction (see Figure 3) into 5  $\mu\text{m}$  thick slices spaced by 50-100  $\mu\text{m}$ . Each slice is stained with Movat's Pentachrome such that the collagen-rich fibrosa appears yellow, the spongiosa appears blue, and the elastin-rich ventricularis appears black. The cell nuclei of each layer also stain black. The slices are mounted on glass slides for bright-field microscopic imaging.

Image capturing is done with a CCD camera mounted on a Leica DMI600B light microscope interfaced with a computer equipped with an image-acquisition software. Along each circumferential slice, separate images are taken in the radial direction at 200  $\mu\text{m}$  intervals. This divides the leaflet by a network of square (200  $\mu\text{m}$  x 200  $\mu\text{m}$ ) grids. It is also important to have a numerical organization system such that each local image of the leaflet corresponds to its location on the image grid. This will allow for an accurate three-dimensional reconstruction of the entire leaflet. The images are saved in TIFF formats for later image analysis in Image J or an analogous image analysis program. Image J is particularly advantageous because it is open source, allowing the experimenter to modify the program as needed.

After the each leaflet has been imaged according to the aforementioned grid, each image will be imported and analyzed separately in Image J. A representative pre-analysis image is shown in Figure 4. To conduct cytometry, it is important to enhance the contrast such that all the cell nuclei can be visually differentiated from the background. See Figure 5 for the contrast enhancement of Figure 4. After the contrast has been properly adjusted, an intensity threshold must be set for cytometry. This threshold defines the limit of the intensity that differentiates a cell nucleus from surrounding background noise. After setting the threshold the image is converted into a purely binary, black-and-white image. See Figure 6. To quantify the number of cell nuclei in each image, the Analyze Particles function will be used. Each cell nuclei is identified according to three criteria: the aforementioned contrast-threshold, its size, and circularity. Size and circularity selection excludes debris particles or elastin fibers that are either too small, too large, or doesn't fit the ellipsoid shape of a cell nucleus. These characterization criterion are sufficient given that no overlap exist between cell nuclei. Since the cells being examined are relatively large in terms of cytoplasmic volume and the density of the cells is fairly sparse, this assumption holds up well. The size and the circularity setting for the nuclei particles within a consistent range given magnification power stay the same and the slices are from the same leaflet. Figure 7 shows the complete cytometric analysis performed on Figure 4. A comparison between Figure 4 and 7 shows that the Particle Analysis function can accurately produce cytometric measurements.

To measure the layer thickness, the user must calibrate Image J using a line of known distance. This can be done by incorporate a scaling line of known length (in terms of units of actual length) into the initial image acquired during microscopy. Then the Scale function in Image J can be used to measure the length of the scaling line in units of pixels. Thus a calibration is established between

actually length and the number of pixels. The user is then free to use the length measurement tool in Image J to measure the thickness of each of three cell layers.

### **Possible Results and Future Directive**

Given the timeframe of this project, it is reasonable to expect the completion of the cytometry and layer thickness characterization. To complete the digital three-dimensional aortic valve leaflet reconstruction, further image analysis must be done to quantify the amount of collagen and elastin fibers for each layer. This can be done by calling upon the particle analysis function in Image J again. However, instead of identifying circular nuclei, the function looks for the non-circular fibers and quantifies them by area. Alternatively, one could program an algorithm that performs the image analysis by the differential staining of collagen and elastin. After these quantitative analyses, the stacks function in Image J or some other three-dimensional rendering program could be used to piece together the slices to complete a volumetric representation of the entire leaflet. The completed volumetric rendering could incorporate simulation algorithms that model the bio-mechanical response of leaflet and allow for the investigation of the leaflet microstructure under dynamic conditions.

**Attachments**

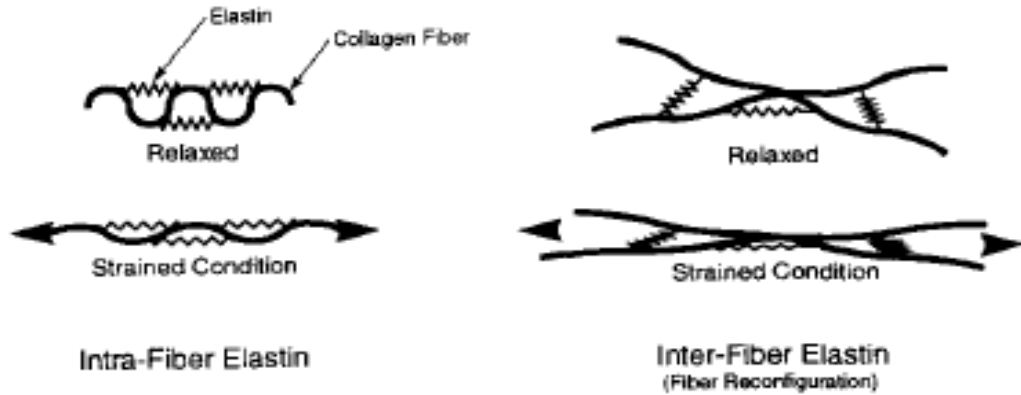


**Figure 1.** Proposed microstructure of the aortic valve giving it unique stiffness and elasticity. [4]

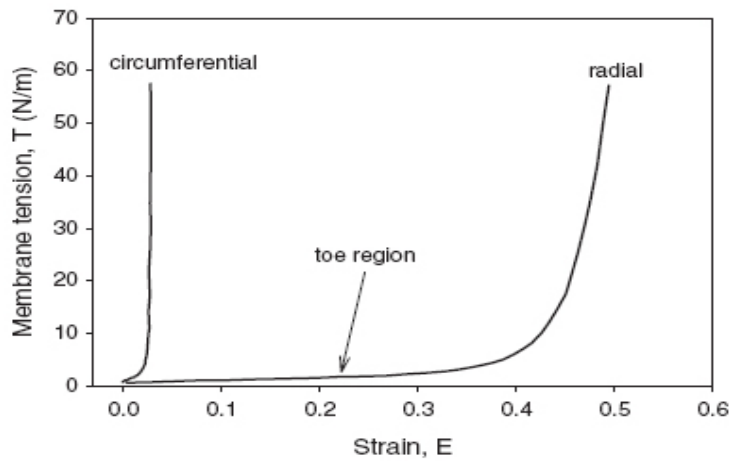


**Figure 2.** Stress-strain relationship of a 10 mm x10 mm native porcine aortic valve leaflet. [1]



**Figure 3.** Aortic valve leaflet.

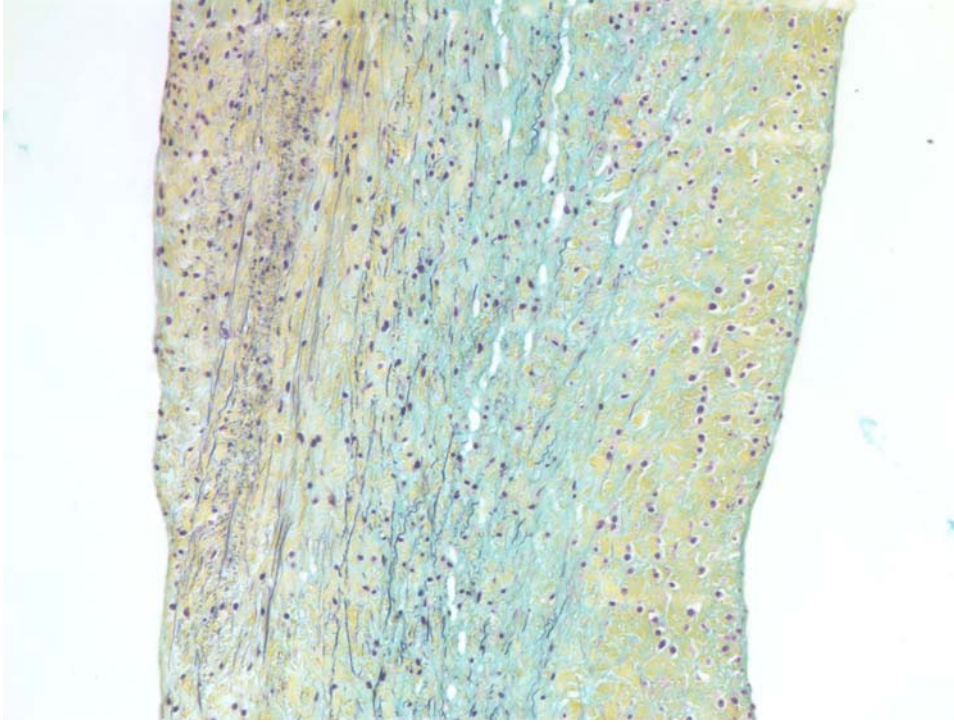


**Figure 4.** Non-enhanced radial slice of the aortic valve leaflet. Collagen fibers are running out of the plane of the page in the fibrosa where elastin fibers are running vertically in the plane of the page in the ventricularis.

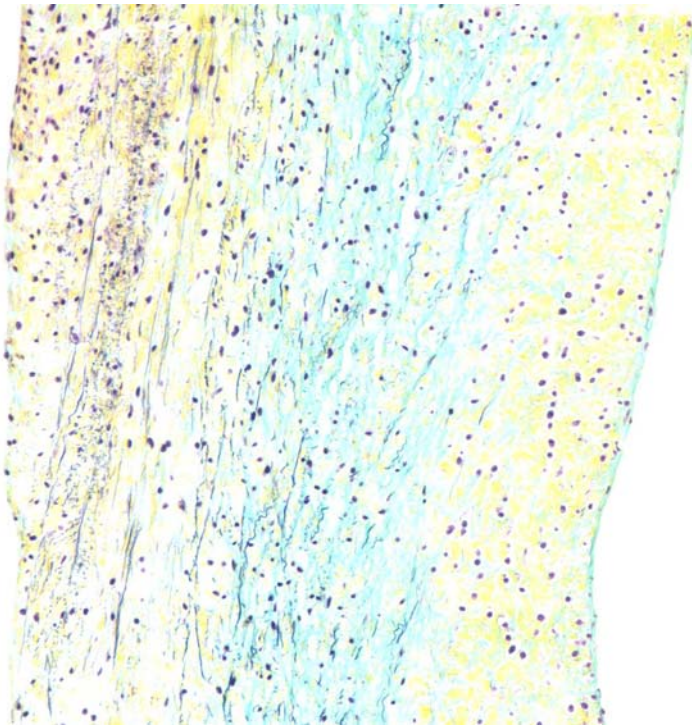


**Figure 5.** Figure 4 after contrast enhancement.





**Figure 6.** Threshold setting for Figure 5.

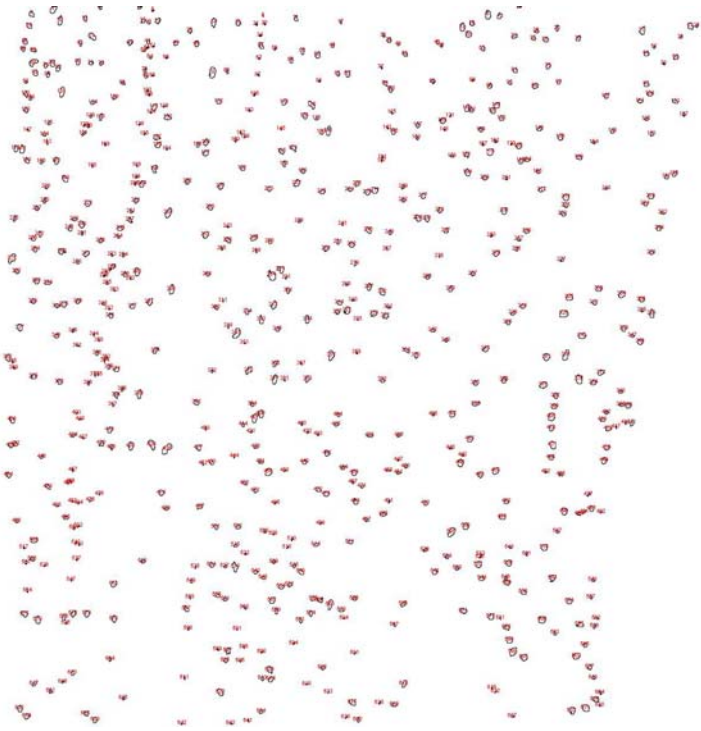


**Figure 7.** Particle analysis of Figure 6 where all fibers are excluded by the ellipsoid fitting function of Image J.

## Citations

[1.] Merryman, W.D., Engelmayer Jr., G.C., et al. Defining biomechanical endpoints for tissue engineered heart valve leaflets from native leaflet properties. *Progress in Pediatric Cardiology*. 2006. 21:153-160

[2.] Sacks, M.S. Biomechanics of native and engineered heart valve tissues. A chapter in Functional Tissue Engineering: The Role of Biomechanics. Edited by Guilak, Butler, Mooney, and Goldstein. 2001.

[3.] Bender M.D., J.R. Heart valve disease. Chapter 13 in Yale University School of Medicine Heart Book. 1992

[4.] Scott, M. and Vesely, I. Aortic valve cusp microstructure: the role of elastin. *Ann. Thorac. Surg.* 1995. 60:S391-4.

[5.] Vesely, I. The role of elastin in aortic valve mechanics. *Journal of Biomechanics* 1998. 31:115-123.